Seed-produced anti-globulin VHH-Fc antibodies retrieve globulin precursors in the insoluble fraction and modulate the *Arabidopsis thaliana* seed subcellular morphology

Thomas De Meyer[1,2,‡], Elsa Arcalis[3,‡], Stanislav Melnik[3], Katrien Maleux[1,2], Jonah Nolf[1,2], Friedrich Altmann[4], Ann Depicker[1,2,*] and Eva Stoger[3,*]

[1] *VIB Center for Plant Systems Biology, B-9052 Ghent, Belgium,*

[2] *Department of Plant Biotechnology and Bioinformatics, Ghent University, B-9052 Ghent, Belgium,*

[3] *Department of Applied Genetics and Cell Biology, University of Natural Resources and Plant Sciences, Vienna, Austria and*

[4] *Department of Chemistry, University of Natural Resources and Life Sciences, Vienna, Austria*

[*]For correspondence (emails anna.depicker@ugent.be and eva.stoeger@boku.ac.at).

[‡]These authors contributed equally to this work.

Corresponding authors:

Ann Depicker

Department Plant Biotechnology and Bioinformatics
Ghent University
Technologiepark 71
B-9052 Gent, Belgium
Tel: +32 9 331 39 47

Eva Stöger

Department of Applied Genetics and Cell Biology BOKU
University of Natural Resources and Life Sciences
Muthgasse 18
1190 Vienna , Austria
Tel: +43 1 47654-94111

Running title: Antibodies against globulin seed storage protein

Key message

Nanobody-heavy chain (VHH-Fc) antibody formats have the potential to immunomodulate even highly accumulating proteins and provide a valuable tool to modulate the subcellular distribution of seed storage proteins experimentally.

Abstract

Recombinant antibodies often obtain high accumulation levels in plants, and thus, besides being the actual end-product, antibodies targeting endogenous host proteins can be used to interfere with the localization and functioning of their corresponding antigens. Here, we compared the effect of a seed-expressed nanobody-heavy chain (VHH-Fc) antibody against the highly abundant *Arabidopsis thaliana* globulin seed storage protein cruciferin with that of a VHH-Fc antibody without endogenous target. Both antibodies reached high accumulation levels of around 10% of total soluble protein, but strikingly, another significant part was present in the insoluble protein fraction and was recovered only after denaturing extraction. In seeds containing the anti-cruciferin antibodies and not in seeds containing the antibody without endogenous target, the amount of soluble, processed globulin subunits was severely reduced and a major part of the cruciferin molecules was found as precursor in the insoluble fraction. Moreover, in these seeds, aberrant vacuolar phenotypes were observed that were different from the effects caused by the depletion of globulins in knock-out seeds. Remarkably, the seeds with strongly reduced globulin amounts are fully viable and germinate with frequencies similar to wild type, illustrating how flexible seeds can retrieve amino acids from the stored proteins to start germination.

Keywords Protein storage vacuole; Seed storage protein; Russell-like bodies; VHH-Fc fusions; Immunomodulation; Molecular farming

Introduction

Antibodies are not only considered the actual end-product of protein production for diagnostic or therapeutic purposes, they have also been evaluated as immunomodulators or 'protein silencers' to interfere with biological processes. In this approach, antibodies can prevent proper functioning, trafficking and folding of their corresponding antigen *in vivo* (De Jaeger et al. 2000; Conrad and Manteuffel 2001; Gahrtz and Conrad 2009). The prerequisites for successful immunomodulation are sufficiently high antibody levels as compared to those of the antigen, stable and functional accumulation in a particular cellular compartment, effective binding to epitopes that enable the pursued type of modulation, and high affinity, especially when the antibody needs to compete with endogenous interacting proteins.

Until now in plants, single-chain variable fragments (scFvs) have been the preferred antibody format for introducing novel phenotypes. They were mainly expressed to confer plant resistance against fungal pathogens (Peschen et al. 2004; Yajima et al. 2010; Brar and Bhattacharyya 2012; Cheng et al. 2015), viruses (Tavladoraki et al. 1993; Fecker et al. 1997; Zimmermann et al. 1998; Boonrod et al. 2004; Villani et al. 2005; Nickel et al. 2008; Cervera et al. 2010), herbicides (Eto et al. 2003; Almquist et al. 2004; Horsman et al. 2007) and bacteria (Malembic-Maher et al. 2005) or to interfere with plant hormones, such as gibberellin (Suzuki et al. 2008; Urakami et al. 2008), abscisic acid (Artsaenko et al. 1995), jasmonic acid (ten Hoopen et al. 2007), auxin (Leblanc et al. 1999) and cytokinin (Zábrady et al. 2014). Hormonal interference can be achieved with scFvs against components of the hormone-signaling cascade. Alternatively, cytoplasmic scFvs targeting a hormone precursor or the actual bioactive hormone can prevent hormone biosynthesis or the subsequent hormone-receptor interaction, respectively. However, functional scFvs have not always been successfully obtained in the reducing cytoplasmic environment (Xiao et al. 2000; Eto et al. 2003; Malembic-Maher et al. 2005) and have not always led to a detectable phenotype (Santos et al. 2004). A workflow to select appropriate scFvs for *in vivo* application has been described by Zábrady et al. (2014).

VHHs or nanobodies, which are the N-terminal antigen-binding domain of camelid heavy-chain antibodies, are also used as immunomodulational agents in plants because of their capability of binding distinct, non-conventional epitopes and their high *in vivo* stability (Muyldermans 2013). For example, VHHs have been developed against auxin (Sheedy et al. 2006), *broad bean mottle virus* (Ghannam et al. 2015) and potato starch branching enzyme A (SBE A) (Jobling et al. 2003). The anti-SBE A VHH only accumulated to about 0.03% of total soluble protein (TSP) in potato leaves and tubers, which corresponds to reported VHH levels of <1% in the leaves and seeds of the dicot model plant, *Arabidopsis thaliana* (Winichayakul et al. 2009; De Buck et al. 2013). Because SBE A itself represents about 0.01% of TSP in potato tubers, the low accumulation level of anti-SBE A VHH was sufficient to successfully inhibit SBE A activity, leading to a very high amylose content. In a more recent study, a chimeric nanobody against green fluorescent protein was fused to an F-box domain, which enables protein degradation via the ubiquitin proteasome pathway, and nanobody-guided degradation of the target protein could be demonstrated in tobacco leaves (Baudisch et al. 2018).

Here, we extended the approach of VHH-based immunomodulation by expressing VHH-Fc fusion proteins against highly accumulating plant antigens such as seed storage proteins (SSPs). The Fc tag was added to obtain sufficiently high protein accumulation levels (De Buck et al. 2013) and to enable possible avidity effects in antigen binding and aggregation of multimeric target proteins. As proof of concept, we focused on the *A. thaliana* globulin SSP, which accumulates during seed maturation phase and eventually represents up to 84% of the seed proteome together with the other major SSP, albumin (Baud et al. 2002). Globulin protein synthesis starts by co-translational transport into the endoplasmic reticulum (ER) lumen, followed by trafficking towards the protein storage vacuoles (PSVs) for long-term storage in desiccated, mature seeds. During this trafficking, proteolytic processing starts in the multivesicular bodies and globulin subunits cluster into α_6-ß$_6$ globulin hexamers, mediated by disulfide bridges (Otegui et al. 2006). We show that a globulin-targeting VHH-Fc fusion protein could immunomodulate the accumulation and trafficking of the highly accumulating globulins and interfere with the default SSP deposition pathway.

Materials and methods

Generation of *VHH58-Fc* and *GBP-Fc* expressing *A. thaliana* plants

The workflow starting from VHH-encoding sequence to the selection of transgenic *A. thaliana* seeds expressing dimeric VHH-Fc has been described previously (De Meyer et al. 2015). Briefly, VHH58 was cloned from its pHen6c *E. coli* expression vector (De Meyer et al. 2014) into the pEnV3Fc entry vector. The resulting entry vector was recombined in the pPphasGW destination vector (Morandini et al. 2011) in a Gateway® LR reaction to generate the pPphas-VHH58-Fc expression vector. In this way, VHH58-Fc is regulated by the seed-specific ß-phaseolin promoter of *Phaseolus vulgaris* and fused with an N-terminal 2S2 signal peptide and a C-terminal KDEL-tag for ER retention.

The pPphas-VHH58-Fc expression vector was transformed to heat-shock competent *Agrobacterium tumefaciens* (strain C58C1 Rif^R) for floral dip transformation of *A. thaliana* (De Buck et al. 2012). T1 transgenic seeds were selected by sowing on K1 medium supplemented with kanamycin (50 mg/l) and 20 T1 plants were allowed to self-pollinate to generate T2 seed stocks. T2 seed protein extracts were prepared by crushing the seeds and dissolving the powder in extraction buffer (50 mM TRIS, 200 mM NaCl, 5 mM EDTA, 0.1% Tween20, pH 8, cOmplete® Protease Inhibitor (Roche)) as described by De Meyer et al. (2015). Next, the highest accumulating seed stock was identified by SDS-PAGE and western blot with 1/5000 diluted goat anti-mouse IgG3 antibodies fused with horseradish

peroxidase (Southern Biotech). Accumulation levels of VHH58-Fc were estimated via the Bio-Rad ChemiDocTM Imaging System (Bio-Rad, Hercules, CA).

The GBP-Fc accumulating line used as control and reference was obtained as described in De Meyer et al. (2015).

Germination efficiency of GBP-Fc and VHH58-Fc homozygous T4 seed stocks

Seed stocks were sown and harvested simultaneously. Five homozygous T4 seed stocks of each construct were analyzed, and germination efficiency was assessed by sowing 100 seeds on non-selective K1 medium.

Preparing seed extracts under denaturing conditions

To isolate insoluble seed proteins, first a soluble protein extraction was performed in 20 mM Pi, 300 mM NaCl, 0.1% CHAPS, 5 mM EDTA, pH 7.8 as described by De Meyer et al. (2015). Then, the residual seed pellet was washed three times using the same extraction buffer. Finally, insoluble proteins were extracted with extraction buffer supplemented with 5% ß-mercaptoethanol and 8 M urea.

For Endoglycosidase H digest, Endo H from NEB was used according to the manufacturer's protocol. About 6 µg (soluble fractions) and 1.6 µg (denatured fractions) of total protein were separated on a 4-12% Bis-Tris polyacrylamide gel.

Protein identification by peptide mass fingerprinting

Bands of interest were manually excised into separate samples, destained and subjected to S-carbamidomethylation and in-gel trypsinolysis according to standard protocols (Shevchenko et al. 2006). Peptide samples in 5% formic acid were applied onto a stainless-steel MALDI target together with an equal volume of matrix solution (1% α-cyano-4-hydroxycinnamic acid in 70% acetonitrile and 30% of 0.1% TFA in water) and quickly dried. Mass spectra were acquired on the Autoflex Speed MALDI-TOF/TOF instrument (Bruker) in reflector positive ion mode. Spectra were analyzed by Flex Analysis software v.3.3. The Mascot web-based application (Matrix Science, http://www.matrixscience.com) was used for peptide mass fingerprinting (PMF) via SwissProt database searching for *Arabidopsis thaliana*. The search parameters were set as follows: trypsin as digestion enzyme with 1 allowed missed cleavage, mass tolerance – 80 ppm, carbamidomethylation of cysteines and oxidation of methionines as fixed and variable modifications, respectively. Positive hits were additionally evaluated based on protein molecular weight, peptide coverage, and known post-translational modifications and processing.

Protein in-gel digestion and glycopeptide analysis

The bands were excised from SDS-PAGE and cut into small pieces. Each band was destained, carbamidomethylated and digested with trypsin, as described previously (Kolarich and Altmann 2000; Kolarich et al. 2006). The peptides were separated by capillary reversed-phase chromatography with a Q-TOF Ultima Global mass spectrometer (Waters, Manchester, UK) for detection (Van Droogenbroeck et al. 2007). The MS data from the tryptic peptides were analyzed as previously described (Van Droogenbroeck et al. 2007) and compared with data sets generated by in silico tryptic digestion of the VHH-Fc-encoding region using the PeptideMass program (http://www.expasy.org/tools/peptide-

mass.html). Based on the tryptic peptide data sets, tryptic glycopeptide data sets were generated by the addition of glycan mass increments to the masses of the identified glycopeptides, as previously described (Van Droogenbroeck et al. 2007).

Production of anti-albumin VHH28-hIgG1 antibody

To visualize albumin in the microscopy analyses, albumin-specific antibodies were needed. Therefore, previously generated anti-albumin VHH28 (De Meyer et al. 2014) was fused to human IgG1 Fc to create a dimeric VHH-Fc antibody for transient production in *Nicotiana benthamiana* leaves as described before (De Meyer et al. 2015). Briefly, the pEnVHH28-hIgG1 entry vector was created by replacing the mouse IgG3 Fc sequence in pENVHH28-mIgG3 (De Meyer et al. 2015) with that of human IgG1 (De Buck et al. 2013) using the *Eco*91 and *BamH*I restriction sites. Subsequently, VHH28-hIgG1 was cloned from pENVHH28-hIgG1 into the pEAQ-HT-DEST1 destination vector (Sainsbury et al. 2009), transformed into *A. tumefaciens* strain LBA4404, infiltrated in *N. benthamiana* leaves and protein A-purified.

Confocal microscopy

Isolated embryos of WT seeds as well as embryos expressing *GBP-Fc* and *VHH58-Fc* were stained with neutral red and ER-Tracker Green™ for visualization of the PSVs and the ER, respectively (Feeney et al. 2018; Ibl et al. 2018). Briefly, embryos were incubated with both stains diluted in tap water and immediately mounted in the staining solution. Observations were performed under a Leica TCS SP5 confocal microscope. At least three samples per line, each containing a minimum of five seeds, were analyzed.

Immunofluorescence and electron microscopy of *A. thaliana* seeds

For immunostaining, *Arabidopsis* embryos were fixed in 4% paraformaldehyde and 0.5% glutaraldehyde in 0.1 M phosphate buffer pH 7.4 for 2 h at room temperature. After several washes with 0.1 M phosphate buffer pH 7.4, samples were dehydrated through an ethanol series and then infiltrated and embedded in LR-White resin (Arcalis et al. 2010). One-µm sections were prepared with a Leica Ultracut UCT and collected on glass slides for immunofluorescence. Sections showing silver interferences were collected on copper grids for immunogold labeling. Labeling of the sections was done as previously described (Arcalis et al. 2010). As primary antibodies, polyclonal goat anti-mouse IgG (Sigma), polyclonal rabbit anti-globulin (Shimada et al. 2003) and anti-albumin VHH28-hIgG1 antibodies were used. The antigen-antibody reactions were detected with donkey anti-goat or donkey anti-rabbit sera labeled with Alexa Fluor 488® or 546® (Invitrogen) for fluorescence microscopy. Samples were observed under a Leica DM 5500 fluorescence microscope or a FEI Tecnai G2 electron microscope. At least three samples per line, each containing a minimum of five seeds, were analyzed.

Results

Significant amounts of the recombinant VHH-Fc are insoluble

To investigate the potential of VHH-Fc antibodies to immunomodulate highly accumulating plant antigens, we fused a previously generated globulin-binding VHH, termed VHH58 (De Meyer et al. 2014), to the Fc domain of mouse IgG3, also including an N-terminal 2S2 signal peptide and a C-terminal KDEL-tag for ER retention. This fusion was expressed in *A. thaliana* seeds under the control of the seed-specific ß-phaseolin promoter that is active during the seed maturation phase (De Wilde et al. 2013). A high-accumulating T2 seed stock was identified by SDS-PAGE and immunoblot analysis of seed protein extracts from 20 independent transformants (Supplementary Fig. 1). Subsequently, we generated homozygous T3 and T4 seed stocks, the latter containing VHH58-Fc up to 9.3% of TSP, as determined by western blot.

Next, the VHH58-Fc T4 seed protein extracts were analyzed on SDS-PAGE together with wild-type (WT) seeds and seeds expressing the KDEL-tagged GBP-Fc, an anti-green fluorescent protein VHH also fused to the Fc domain of mouse IgG3, at 13% of TSP (De Meyer et al. 2015). Both VHH58-Fc and GBP-Fc ran as a doublet with a major band of glycosylated and a minor band of non-glycosylated proteins with a molecular weight of about 42 kDa, absent in the WT soluble protein extract (Fig. 1). Because binding of the VHH58-Fc antibodies on the multimeric globulin proteins might result in insoluble aggregates, we also analyzed the content of the pellet fraction and re-extracted it with denaturing extraction buffer. Strikingly, significant amounts of insoluble glycosylated and non-glycosylated VHH-Fc proteins were present in the pellet fraction of not only the VHH58-Fc producing line, but also of the GBP-Fc producing line, in which the antibody does not have a target epitope and is thus expected to be present as a monomer.

VHH58-Fc expressing seeds accumulate cruciferin precursor proteins

A. thaliana ecotype Columbia contains three globulin-encoding genes, namely *CRA1*, *CRU2* and *CRU3*, each of which gives rise to an acidic (α) and basic (ß) globulin subunit. In WT and GBP-Fc seeds, the distinct globulin subunits at ~34 kDa and ~22 kDa were clearly visible in the soluble seed extracts but not in the insoluble fraction (Fig. 1). In contrast, these globulin subunits were severely reduced in the soluble extracts of *VHH58-Fc* expressing seeds (Fig. 1, arrowheads in the first lane). The ~34-kDa band was designated CRU3 by comparing the SDS-PAGE profile with that of double knock-out seeds that only express one of the three globulin genes (Fig. 1) (Withana-Gamage et al. 2013). This was further confirmed by peptide mass fingerprinting (PMF) of the corresponding bands excised from the WT sample. The ~34-kDa band was identified as the α chain, and the ~22-kDa band contained the ß chain of cruciferin C (UniProt ID Q96318; CRU3) (Supplementary Fig. 2). Moreover, three additional higher molecular weight bands appeared in the pellet fraction of the VHH58-Fc seed extract (Fig. 1). These bands were also excised and analyzed by PMF (Supplementary Fig. 2). Peptides in the band with the highest molecular mass of ~56-kDa could be assigned to both the α and ß subunits of cruciferin C, identifying the band as cruciferin C precursor. Peptides of the ~50-kDa band corresponded to cruciferin A1 precursor (UniProt ID P15455; CRA1), and peptides of the ~48-kDa band were assigned to cruciferin B precursor (UniProt ID P15456; CRU2) (Fig. 1 and Supplementary Fig. 2).

Both soluble and insoluble VHH58-Fc carry mostly oligomannosidic N-glycans

Determining the type of N-glycans present on the VHH-Fc molecules can provide valuable information about protein trafficking, e.g. the presence of complex-type N-glycans represents a footprint of processing in the Golgi complex. To

this end, VHH58-Fc and GBP-Fc protein bands, both from the soluble and pellet fraction of the seed extracts, were excised from SDS-PAGE and analyzed by mass spectrometry (MS) (Fig. 2a-d). Soluble VHH58-Fc and GBP-Fc both contained mostly oligomannosidic N-glycans (Man5 to Man9) and only small amounts of complex-type N-glycans (GnGnXF and MGnXF). Similar profiles were obtained for the two respective pellet fractions, indicating that most of the protein found in either fraction did not pass through the Golgi. The MS-based glycopeptide analysis was also confirmed by a digest with Endoglycosidase H (EndoH), revealing that the main part of the glycoprotein in all samples was sensitive to EndoH (Fig. 2e).

GBP-Fc is localized in the protein storage vacuoles (PSVs), apoplast and ER-derived structures, but does not alter SSP distribution

To determine the subcellular effect of anti-globulin *VHH58-Fc* expression, we first examined WT and GBP-Fc seeds by confocal laser scanning microscopy (CLSM), immunofluorescence microscopy, and transmission electron microscopy (TEM). WT cotyledon cells contained several PSVs of different shape and size, but clearly defined by neutral red staining (Supplementary Fig. 3a). The typically electron-dense PSVs (Supplementary Fig. 3b) were filled with globulin and albumin SSPs that perfectly co-localized (Supplementary Fig. 3c-e).

In contrast to WT seeds, abundant membrane-bound structures containing GBP-Fc were observed in transgenic cotyledon cells (Fig. 3b, c; Supplementary Fig. 4). These structures of around 300 nm in size were identified as ER derived because staining with ER-Tracker Green™ revealed a clear distortion of the fine reticulate pattern of the ER in the form of aggregates (Fig. 3a). In spite of carrying a KDEL-tag, GBP-Fc antibodies were also found in the PSVs and in the apoplast (Fig. 3d, e). Of note, PSV localization was not evident from the immunofluorescence microscopy, probably because of masking by the much stronger signal in the apoplast and ER-derived structures (Fig. 3b). The expression of *GBP-Fc* did not alter SSP distribution, because both globulin and albumin were localized in the PSVs (Fig. 3e, f).

VHH58-Fc alters the distribution of globulin and causes distorted PSVs

The deposition pattern of VHH58-Fc antibodies was similar to that of GBP-Fc because abundant ER-derived structures containing VHH-Fcs were observed within the cotyledon cells (Fig. 4b-d), and VHH58-Fc was also found in the apoplast (Fig. 4b, f). Interestingly, VHH58-Fc could be also detected in the cell periphery, forming electron-dense deposits in the periplasmic space (Fig. 4b, c, g and Supplementary Fig. 5). Most notably, the presence of VHH58-Fc induced a clear vacuolar phenotype. Normal PSVs were no longer observed and instead, a scrambled pattern was obtained with neutral red staining (Fig. 4a).

The TEM analysis showed an even more obvious vacuolar phenotype with no electron-dense PSVs but only mere PSV remnants (Fig. 4c, e and Supplementary Fig. 5). The presence of ER-derived structures and a dilated periplasmic space completed the characteristics of this subcellular phenotype (Fig. 4c, g). Interestingly, the peculiar subcellular organization of VHH58-Fc seeds did not lead to a reduced seed germination efficiency compared to GBP-Fc seeds (Supplementary Fig. 6).

Given the strong distortion in the endomembrane compartments of the cotyledon cells, we next checked VHH-Fc and SSP distribution. Both VHH58-Fc and globulin were localized to the PSV remnants, apoplast, ER-derived

structures and the periplasmic space (Fig. 4d, e,h). Albumin remained restricted to the PSVs (Fig. 4i, j). Of note, the microscopy experiments were confirmed by analysis of a second transformant to exclude potential T-DNA position effects (Supplementary Fig. 5).

To find out if the strong vacuolar phenotype was due to globulin depletion in the PSV, we analyzed triple globulin *cra1cru2cru3* knock-out seeds (Withana-Gamage et al. 2013) by TEM. The PSVs appeared slightly smaller, but no significant ultrastructural changes were found (Supplementary Fig. 7), well in agreement with Withana-Gamage et al. (2013). Immunolocalization confirmed specific labeling for albumin within the PSVs, but no significant labeling for globulins was found in the triple *cra1cru2cru3* mutant (Supplementary Fig. 7).

Discussion

High VHH-Fc accumulation is thought to induce the formation of Russell-like bodies

GBP-Fc and VHH58-Fc were mainly localized in ER-derived structures and in the apoplast, and to a lesser extent also in PSVs. Similar observations have previously been made for other KDEL-tagged proteins (De Meyer and Depicker 2014). However, the cause of the observed ER leakage to the apoplast is unknown, especially because we previously demonstrated the intactness of the GBP-Fc KDEL-tag by LC-MS/MS (De Meyer et al. 2015). Possibly, the GBP-Fc molecule is folded in such a way that the KDEL-tag is less accessible. Both VHH-Fc antibodies induced the formation of ER-derived structures, which are thought to arise from a local build-up of KDEL-tagged proteins in the ER that overwhelms the ER storage capacity. Several recombinant chimeric antibody formats involving an Fc-fusion have previously been reported to be partially localized in ER-derived structures in *Arabidopsis* seeds (Van Droogenbroeck et al. 2007; Loos et al. 2011). More recently, we could show that the production of murine interleukin-10 in *Arabidopsis thaliana* seeds resulted in the formation of ER-derived structures containing a large fraction of the recombinant protein in an insoluble form. Since these ER-derived structures resemble mammalian Russell bodies in many ways we suggested the term “Russell-like bodies” (Arcalis et al. 2019). In the same study, *Arabidopsis* seeds expressing scFv-Fc antibodies MBP-10, Hep78A and EHF34 (Van Droogenbroeck et al. 2007) were re-examined, and for each of these antibodies, a significant portion was insoluble in non-ionic detergent. Therefore, the formation of insoluble aggregates and Russell-like bodies upon overexpression of recombinant proteins seems a common phenomenon, although this has rarely been investigated in detail and may sometimes not even be noticed. It is also interesting to point out that the N-glycan patterns did not differ between the soluble and the insoluble VHH-Fc fractions, suggesting that the formation of insoluble aggregates was not due to the presence or lack of a specific N-glycan structure, nor linked to a specific subcellular transport route.

Here, the overall N-glycan pattern of the VHH-Fc antibodies was determined to find out if their deposition in the distinct subcellular compartments is reflected in their N-glycan structures. Both GBP-Fc and VHH58-Fc contained mostly oligomannosidic N-glycans, with only a minor contribution of Golgi-mediated complex-type modifications. Notably, the relative amounts of N-glycan forms determined in the present study are not in full agreement with our previous analysis, in which it was concluded that GBP-Fc was mainly occupied with complex-type N-glycans (De Meyer et al. 2015). A possible explanation for this discrepancy could be that the former analysis was carried out by capillary electrophoresis following an enzymatic release of the sugar moieties, whereas in the present study, IgG glycopeptides were analyzed by mass spectrometry. A digest with EndoH in the present study clearly confirmed that

oligomannosidic glycans dominate in the soluble as well as the insoluble fraction of GBP-Fc, much in line with the MS analysis. We surmise that in the previous analysis co-purifying endogenous glycoproteins may have contributed to the released sugar pool causing an overestimation of the proportion of complex glycans. Due to its higher specificity, glycopeptide-based analysis is more reliable.

Globulin-binding VHH58-Fc antibodies prevent normal globulin maturation and storage

VHH58-Fc and GBP-Fc antibodies reached comparable accumulation levels, but interestingly, only in the pellet fraction of the VHH58-Fc seed extracts a complete shift from fully processed, soluble globulin subunits to partially processed cruciferin precursors was observed. This suggests that the interaction of the globulin precursor with VHH58-Fc strongly affects globulin processing and/or folding. Indeed, binding of VHH58 to CRA1, CRU2 and CRU3 subunits as well as to globulin precursor proteins has previously been demonstrated (De Meyer et al. 2014). Presumably, the interaction between the VHH58-Fc antibodies and the globulin precursors initiates already in the ER, from where globulin-VHH58-Fc complexes shuttle to distinct subcellular compartments. Large amounts of both VHH58-Fc and globulin were detected in the apoplast, ER-derived structures and periplasmic space. The latter localization was also observed for scFv-Fc antibodies in *A. thaliana* seeds (Van Droogenbroeck et al. 2007). The authors reported that secretion of KDEL-tagged proteins to the periplasmic space was considered an ER saturation effect because the scFv-Fc antibodies carried oligomannosidic N-glycans, and two ER-resident proteins, BiP and calreticulin, were also present in this compartment. In a similar process, the VHH58-Fc antibody might mediate the clustering of globulin molecules in the ER and trigger their secretion to the periplasmic space, which is supported by the mainly oligomannosidic N-glycan pattern of VHH58-Fc. Van Droogenbroeck et al. (2007) also reported that in the scFv-Fc producing seeds, some of the cruciferin was mislocalized to the periplasmic space as a result of a general disturbance of SSP distribution caused by the high levels of recombinant antibody. However, it is important to note that a detailed examination of these seeds did not reveal significant amounts of globulin precursor molecules in the soluble or pellet fraction of the seed extracts (Arcalis et al. 2019). Also the GBP-Fc containing seeds did not contain significant amounts of mislocalized cruciferin. From this, we can conclude that the massive effect of a defect in globulin processing and localization observed in the present study can clearly be attributed to the binding specificity of VHH58-Fc.

Although some globulin was still present inside the PSVs, the PSVs were severely malformed and only PSV remnants were observed. However, it is unlikely that the strong vacuolar phenotype is due to globulin depletion in the PSV, because triple globulin *cra1cru2cru3* knock-out seeds did not show significant ultrastructural changes, well in agreement with the report of Withana-Gamage et al. (2013). Similarly, the α*vpe-1*/β*vpe-3*/γ*vpe-1* mutant, which shows defects in the vacuolar processing enzyme, resulting in massive globulin precursor accumulation, also does not show a visible vacuolar phenotype (Shimada et al. 2003). Consequently, the vacuolar phenotype observed in the current study does not seem to be simply due to a lack of globulin in the PSV, nor due to the lack of globulin processing, but it appears to be a consequence of the globulin precursor being bound and mislocalized by the antibody. Alternatively, the VHH58-Fc antibodies may bind a particular globulin epitope and hence prevent efficient stacking of globulin in PSVs. Strikingly, the malformation of PSVs did not lead to a reduction in seed germination efficiency, pointing to the versatility of seeds. Similarly tobacco seeds, in which the accumulation of 12S globulins was dramatically reduced by immunomodulation of ABA activity, were viable and showed precocious germination (Phillips et al. 1997). Possibly,

the recombinant antibodies, together with the albumin and remaining globulin, represent the building blocks for the growing seedling instead.

Of note, the albumin accumulation levels and their PSV-specific localization were not affected by *VHH58-Fc* expression, highlighting the antibody's specificity towards the globulin SSP. Albumin stability was also described in the globulin *cra1cru2cru3* triple knock-out seeds, in which the lack of globulin was compensated by an increased level of unknown seed proteins other than albumin (Withana-Gamage et al. 2013).

Concluding remarks

In conclusion, by producing anti-globulin VHH58-Fc in *A. thaliana* seeds and studying the seed subcellular morphology, we demonstrated that VHH-Fc antibody formats can interfere with the normal trafficking of highly accumulating endogenous proteins and thereby modify the morphology of storage organelles and SSP distribution in a way that is different from the effects caused by the mere depletion (knock-out) of single components. In seed crops such as cereals, the spatial control of SSP deposition has implications on quality parameters: depending on the species, protein bodies form aggregates either within or outside the PSV and, with progressing seed desiccation, these aggregates fuse to form a protein matrix that is in intimate contact with the starch granules (Wu and Messing 2010). The spatial composition of this matrix defines key agronomic quality traits such as grain hardness (Wu et al. 2010). Several opaque maize mutants have been identified with kernel properties that reflect changes in protein body morphology and size (in some cases even without significant changes in overall protein composition). Although a link between the respective genes and the phenotype has been established, the physical principles that determine the grain morphology are not fully understood (Wang et al. 2012). VHH-Fc antibody formats may provide a valuable tool to modulate the subcellular SSP distribution experimentally to determine the spatial influence of specific SSPs on the overall seed phenotype.

Acknowledgements The authors thank Annick Bleys for help in preparing the manuscript, Thomas Maggen for technical assistance, Prof. Ikuko Hara-Nishimura for the rabbit anti-globulin antibodies, Janitha Wanasundara and Dwayne Hegedus for the globulin knock-out lines and Prof. George Lomonosoff for the pEAQ-HT-DEST1 destination vector. TDM was indebted to the Agency for Innovation by Science and Technology (IWT) for a predoctoral fellowship. We also thank the European Cooperation in Science and Technology (COST) action FA0804 for conference reimbursements. The work was supported by a VIB fund for translational research and the Austrian Science Fund FWF (I2823-B25).

Author contributions

TDM, EA, AD and ES designed the study. TDM, EA, AD and ES wrote the manuscript. TDM, EA, SM, KM, JN and FA performed the experiments. TDM and EA carried out analyses. AD and ES coordinated the project.

Conflicts of interest

The authors declare that there is no conflict of interests regarding the publication of this paper.

References

Almquist KC, Niu Y, McLean MD, Mena FL, Yau KYF, Brown K, Brandle JE, Hall JC (2004) Immunomodulation confers herbicide resistance in plants. Plant Biotechnol J 2:189-197.

Arcalis E, Ibl V, Hilscher J, Rademacher T, Avesani L, Morandini F, Bortesi L, Pezzotti M, Vitale A, Pum D, De Meyer T, Depicker A, Stöger E (2019) Russell-like bodies in plant seeds share common features with prolamin bodies and occur upon recombinant protein production. Front Plant Sci 10:777.

Arcalis E, Stadlmann J, Marcel S, Drakakaki G, Winter V, Rodriguez J, Fischer R, Altmann F, Stoger E (2010) The changing fate of a secretory glycoprotein in developing maize endosperm. Plant Physiol 153:693-702.

Artsaenko O, Peisker M, zur Nieden U, Fiedler U, Weiler EW, Müntz K, Conrad U (1995) Expression of a single-chain Fv antibody against abscisic acid creates a wilty phenotype in transgenic tobacco. Plant J 8:745-750.

Baud S, Boutin J-P, Miquel M, Lepiniec L, Rochat C (2002) An integrated overview of seed development in *Arabidopsis thaliana* ecotype WS. Plant Physiol Biochem 40:151-160.

Baudisch B, Pfort I, Sorge E, Conrad U (2018) Nanobody-directed specific degradation of proteins by the 26S-proteasome in plants. Front Plant Sci 9:130.

Boonrod KJ, Galetzka D, Nagy PD, Conrad U, Krczal G (2004) Single-chain antibodies against a plant viral RNA-dependent RNA polymerase confer virus resistance. Nat Biotechnol 22:856-862.

Brar HK, Bhattacharyya MK (2012) Expression of a single-chain variable-fragment antibody against a *Fusarium virguliforme* toxin peptide enhances tolerance to sudden death syndrome in transgenic soybean plants. Mol Plant-Microbe Interact 25:817-824.

Cervera M, Esteban O, Gil M, Gorris MT, Martínez MC, Peña L, Cambra M (2010) Transgenic expression in citrus of single-chain antibody fragments specific to *Citrus tristeza* virus confers virus resistance. Transgenic Res 19:1001-1015.

Cheng W, Li H-P, Zhang J-B, Du H-J, Wei Q-Y, Huang T, Yang P, Kong X-W, Liao Y-C (2015) Tissue-specific and pathogen-inducible expression of a fusion protein containing a *Fusarium*-specific antibody and a fungal chitinase protects wheat against *Fusarium* pathogens and mycotoxins. Plant Biotechnol J 13:664-674.

Conrad U, Manteuffel R (2001) Immunomodulation of phytohormones and functional proteins in plant cells. Trends Plant Sci 6:399-402.

De Buck S, Nolf J, De Meyer T, Virdi V, De Wilde K, Van Lerberge E, Van Droogenbroeck B, Depicker A (2013) Fusion of an Fc chain to a VHH boosts the accumulation levels in *Arabidopsis* seeds. Plant Biotechnol J 11:1006-1016.

De Buck S, Virdi V, De Meyer T, De Wilde K, Piron R, Nolf J, Van Lerberge E, De Paepe A, Depicker A (2012) Production of camel-like antibodies in plants. Methods Mol Biol 911:305-324.

De Jaeger G, De Wilde C, Eeckhout D, Fiers E, Depicker A (2000) The plantibody approach: expression of antibody genes in plants to modulate plant metabolism or to obtain pathogen resistance. Plant Mol Biol 43:419-428.

De Meyer T, Depicker A (2014) Trafficking of endoplasmic reticulum-retained recombinant proteins is unpredictable in *Arabidopsis thaliana*. Front Plant Sci 5:473.

De Meyer T, Eeckhout D, De Rycke R, De Buck S, Muyldermans S, Depicker A (2014) Generation of VHH antibodies against the *Arabidopsis thaliana* seed storage proteins. Plant Mol Biol 84:83-93.

De Meyer T, Laukens B, Nolf J, Van Lerberge E, De Rycke R, De Beuckelaer A, De Buck S, Callewaert N, Depicker A (2015) Comparison of VHH-Fc antibody production in *Arabidopsis thaliana*, *Nicotiana benthamiana* and *Pichia pastoris*. Plant Biotechnol J 13:938-947.

De Wilde K, De Buck S, Vanneste K, Depicker A (2013) Recombinant antibody production in Arabidopsis seeds triggers an unfolded protein response. Plant Physiol 161:1021-1033.

Eto J, Suzuki Y, Ohkawa H, Yamaguchi I (2003) Anti-herbicide single-chain antibody expression confers herbicide tolerance in transgenic plants. FEBS Lett 550:179-184.

Fecker LF, Koenig R, Obermeier C (1997) *Nicotiana benthamiana* plants expressing beet necrotic yellow vein virus (BNYVV) coat protein-specific scFv are partially protected against the establishment of the virus in the early stages of infection and its pathogenic effects in the late stages of infection. Arch Virol 142:1857-1863.

Feeney M, Kittelmann M, Menassa R, Hawes C, Frigerio L (2018) Protein storage vacuoles originate from remodeled preexisting vacuoles in *Arabidopsis thaliana*. Plant Physiol 177:241-254.

Gahrtz M, Conrad U (2009) Immunomodulation of plant function by in vitro selected single-chain Fv intrabodies. Methods Mol Biol 483:289-312.

Ghannam A, Kumari S, Muyldermans S, Abbady AQ (2015) Camelid nanobodies with high affinity for *broad bean mottle virus*: a possible promising tool to immunomodulate plant resistance against viruses. Plant Mol Biol 87:355-369.

Horsman J, McLean MD, Olea-Popelka FC, Hall JC (2007) Picloram resistance in transgenic tobacco expressing an anti-picloram scFv antibody is due to reduced translocation. J Agric Food Chem 55:106-112.

Ibl V, Peters J, Stöger E, Arcalis E (2018) Imaging the ER and endomembrane system in cereal endosperm. Methods Mol Biol 1691:251-262.

Jobling SA, Jarman C, Teh M-M, Holmberg N, Blake C, Verhoeyen ME (2003) Immunomodulation of enzyme function in plants by single-domain antibody fragments. Nat Biotechnol 21:77-80.

Kolarich D, Altmann F (2000) *N*-Glycan analysis by matrix-assisted laser desorption/ionization mass spectrometry of electrophoretically separated nonmammalian proteins: application to peanut allergen Ara h 1 and olive pollen allergen Ole e 1. Anal Biochem 285:64-75.

Kolarich D, Turecek PL, Weber A, Mitterer A, Graninger M, Matthiessen P, Nicolaes GAF, Altmann F, Schwarz HP (2006) Biochemical, molecular characterization, and glycoproteomic analyses of α1-proteinase inhibitor products used for replacement therapy. Transfusion 46:1959-1977.

Leblanc N, David K, Grosclaude J, Pradier J-M, Barbier-Brygoo H, Labiau S, Perrot-Rechenmann C (1999) A novel immunological approach establishes that the auxin-binding protein, Nt-abp1, is an element involved in auxin signaling at the plasma membrane. J Biol Chem 274:28314-28320.

Loos A, Van Droogenbroeck B, Hillmer S, Grass J, Pabst M, Castilho A, Kunert R, Liang M, Arcalis E, Robinson DG, Depicker A, Steinkellner H (2011) Expression of antibody fragments with a controlled *N*-glycosylation pattern and induction of endoplasmic reticulum-derived vesicles in seeds of Arabidopsis. Plant Physiol 155:2036-2048.

Malembic-Maher S, Le Gall F, Danet J-L, Dorlhac de Borne F, Bové J-M, Garnier-Semancik M (2005) Transformation of tobacco plants for single-chain antibody expression via apoplastic and symplasmic routes, and analysis of their susceptibility to stolbur phytoplasma infection. Plant Sci 168:349-358.

Morandini F, Avesani L, Bortesi L, Van Droogenbroeck B, De Wilde K, Arcalis E, Bazzoni F, Santi L, Brozzetti A, Falorni A, Stoger E, Depicker A, Pezzotti M (2011) Non-food/feed seeds as biofactories for the high-yield production of recombinant pharmaceuticals. Plant Biotechnol J 9:911-921.

Muyldermans S (2013) Nanobodies: natural single-domain antibodies. Annu Rev Biochem 82:775-797.

Nickel H, Kawchuk L, Twyman RM, Zimmermann S, Junghans H, Winter S, Fischer R, Prüfer D (2008) Plantibody-mediated inhibition of the *Potato leafroll virus* P1 protein reduces virus accumulation. Virus Res 136:140-145.

Otegui MS, Herder R, Schulze J, Jung R, Staehelin LA (2006) The proteolytic processing of seed storage proteins in *Arabidopsis* embryo cells starts in the multivesicular bodies. Plant Cell 18:2567-2581.

Peschen D, Li H-P, Fischer R, Kreuzaler F, Liao Y-C (2004) Fusion proteins comprising a *Fusarium*-specific antibody linked to antifungal peptides protect plants against a fungal pathogen. Nat Biotechnol 22:732-738.

Phillips J, Artsaenko O, Fiedler U, Horstmann C, Mock H-P, Müntz K, Conrad U (1997) Seed-specific immunomodulation of abscisic acid activity induces a developmental switch. EMBO J 16:4489-4496.

Sainsbury F, Thuenemann EC, Lomonossoff GP (2009) pEAQ: versatile expression vectors for easy and quick transient expression of heterologous proteins in plants. Plant Biotechnol J 7:682-693.

Santos MO, Crosby WL, Winkel BSJ (2004) Modulation of flavonoid metabolism in *Arabidopsis* using a phage-derived antibody. Mol Breeding 13:333-343.

Sheedy C, Yau KYF, Hirama T, MacKenzie CR, Hall JC (2006) Selection, characterization, and CDR shuffling of naive llama single-domain antibodies selected against auxin and their cross-reactivity with auxinic herbicides from four chemical families. J Agric Food Chem 54:3668-3678.

Shevchenko A, Tomas H, Havlis J, Olsen JV, Mann M (2006) In-gel digestion for mass spectrometric characterization of proteins and proteomes. Nat Protoc 1:2856-2860.

Shimada T, Yamada K, Kataoka M, Nakaune S, Koumoto Y, Kuroyanagi M, Tabata S, Kato T, Shinozaki K, Seki M, Kobayashi M, Kondo M, Nishimura M, Hara-Nishimura I (2003) Vacuolar processing enzymes are essential for proper processing of seed storage proteins in *Arabidopsis thaliana*. J Biol Chem 278:32292-32299.

Suzuki Y, Mizuno T, Urakami E, Yamaguchi I, Asami T (2008) Immunomodulation of bioactive gibberellin confers gibberellin-deficient phenotypes in plants. Plant Biotechnol J 6:355-367.

Tavladoraki P, Benvenuto E, Trinca S, De Martinis D, Cattaneo A, Galeffi P (1993) Transgenic plants expressing a functional single-chain Fv antibody are specifically protected from virus attack. Nature 366:469-472.

ten Hoopen P, Hunger A, Müller A, Hause B, Kramell R, Wasternack C, Rosahl S, Conrad U (2007) Immunomodulation of jasmonate to manipulate the wound response. J Exp Bot 58:2525-2535.

Urakami E, Yamaguchi I, Asami T, Conrad U, Suzuki Y (2008) Immunomodulation of gibberellin biosynthesis using an anti-precursor gibberellin antibody confers gibberellin-deficient phenotypes. Planta 228:863-873.

Van Droogenbroeck B, Cao J, Stadlmann J, Altmann F, Colanesi S, Hillmer S, Robinson DG, Van Lerberge E, Terryn N, Van Montagu M, Liang M, Depicker A, De Jaeger G (2007) Aberrant localization and underglycosylation of highly accumulating single-chain Fv-Fc antibodies in transgenic *Arabidopsis* seeds. Proc Natl Acad Sci USA 104:1430-1435.

Villani ME, Roggero P, Bitti O, Benvenuto E, Franconi R (2005) Immunomodulation of cucumber mosaic virus infection by intrabodies selected *in vitro* from a stable single-framework phage display library. Plant Mol Biol 58:305-316.

Wang G, Wang F, Wang G, Wang F, Zhang X, Zhong M, Zhang J, Lin D, Tang Y, Xu Z, Song R (2012) *Opaque1* encodes a myosin XI motor protein that is required for endoplasmic reticulum motility and protein body formation in maize endosperm. Plant Cell 24:3447-3462.

Winichayakul S, Pernthaner A, Scott R, Vlaming R, Roberts N (2009) Head-to-tail fusions of camelid antibodies can be expressed *in planta* and bind in rumen fluid. Biotechnol Appl Biochem 53:111-122.

Withana-Gamage TS, Hegedus DD, Qiu X, Yu P, May T, Lydiate D, Wanasundara JPD (2013) Characterization of *Arabidopsis thaliana* lines with altered seed storage protein profiles using synchrotron-powered FT-IR spectromicroscopy. J Agric Food Chem 61:901-912.

Wu Y, Holding DR, Messing J (2010) γ-Zeins are essential for endosperm modification in quality protein maize. Proc Natl Acad Sci USA 107:12810-12815.

Wu Y, Messing J (2010) RNA interference-mediated change in protein body morphology and seed opacity through loss of different zein proteins. Plant Physiol 153:337-347.

Xiao XW, Chu PWG, Frenkel MJ, Tabe LM, Shukla DD, Hanna PJ, Higgins TJV, Müller WJ, Ward CW (2000) Antibody-mediated improved resistance to ClYVV and PVY infections in transgenic tobacco plants expressing a single-chain variable region antibody. Mol Breeding 6:421-431.

Yajima W, Verma SS, Shah S, Rahman MH, Liang Y, Kav NNV (2010) Expression of anti-sclerotinia scFv in transgenic *Brassica napus* enhances tolerance against stem rot. New Biotechnol 27:816-821.

Zábrady M, Hrdinová V, Müller B, Conrad U, Hejátko J, Janda L (2014) Targeted *in vivo* inhibition of specific protein-protein interactions using recombinant antibodies. PLoS ONE 9:e109875.

Zimmermann S, Schillberg S, Liao Y-C, Fisher R (1998) Intracellular expression of TMV-specific single-chain Fv fragments leads to improved virus resistance in *Nicotiana tabacum*. Mol Breeding 4:369-379.

FIGURES

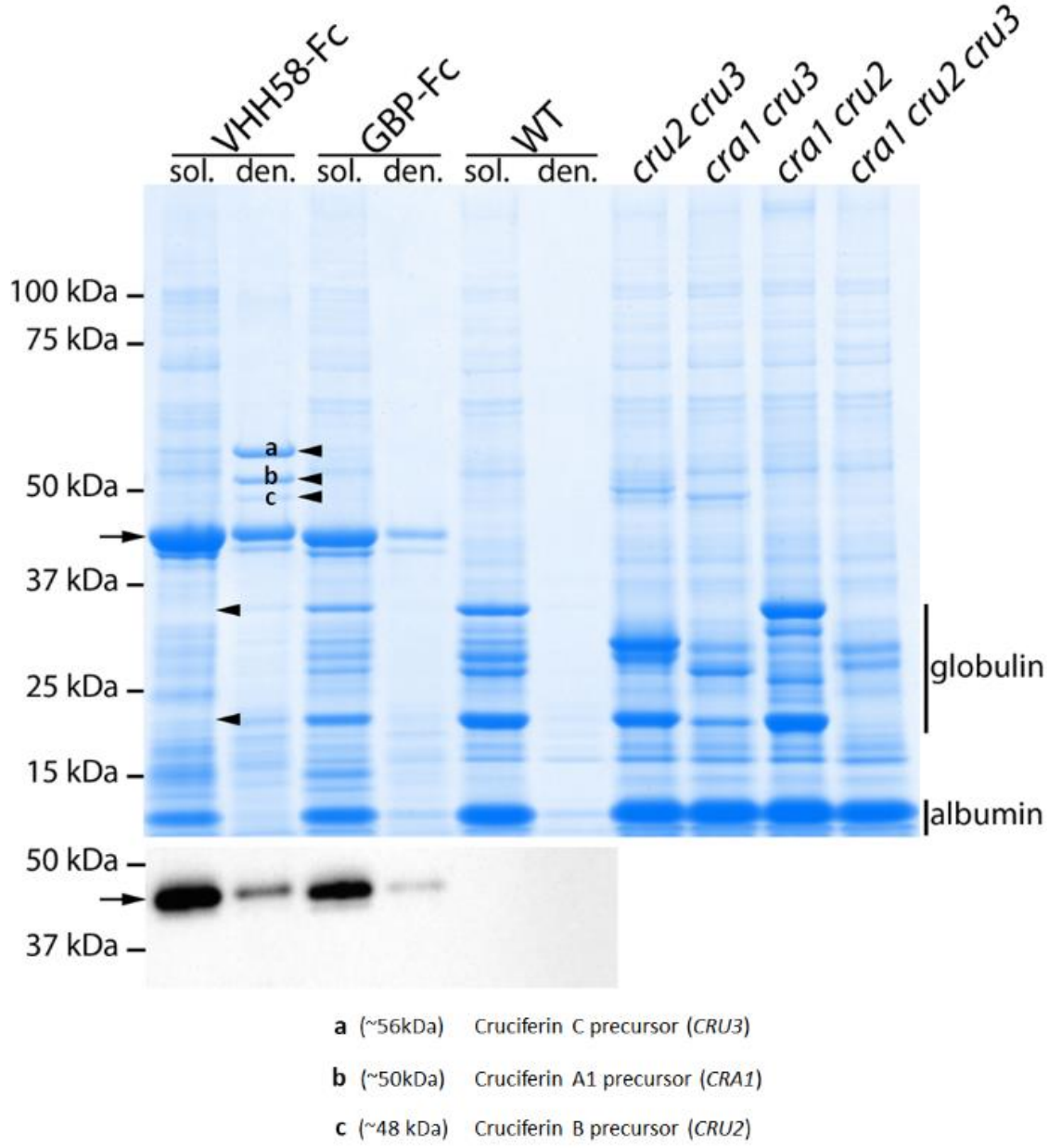

Fig. 1. SDS-PAGE and western blot analysis of VHH-Fc seed extracts. About 32 µg and 3.2 µg of total protein was loaded under reducing conditions for the Coomassie-stained SDS-PAGE (top) and western blot (bottom), respectively. VHH-Fc antibodies at ~42 kDa are indicated with an arrow; the reduced globulin subunits in VHH58-Fc seeds are indicated with arrowheads. The ~34 kDa and ~22 kDa bands marked with arrowheads were identified by PMF as cruciferin C subunits. At the right, the SDS-PAGE profile of protein extracts of double and triple globulin gene knock-out seeds is shown. *sol.* soluble seed extract (extraction was performed in 20 mM Pi, 300 mM NaCl, 0.1% CHAPS, 5 mM EDTA, pH 7.8), *den.* pellet re-extracted under denaturing conditions (extraction buffer supplemented with 5% ß-mercaptoethanol and 8 M urea). Bands designated a, b and c were further identified by PMF.

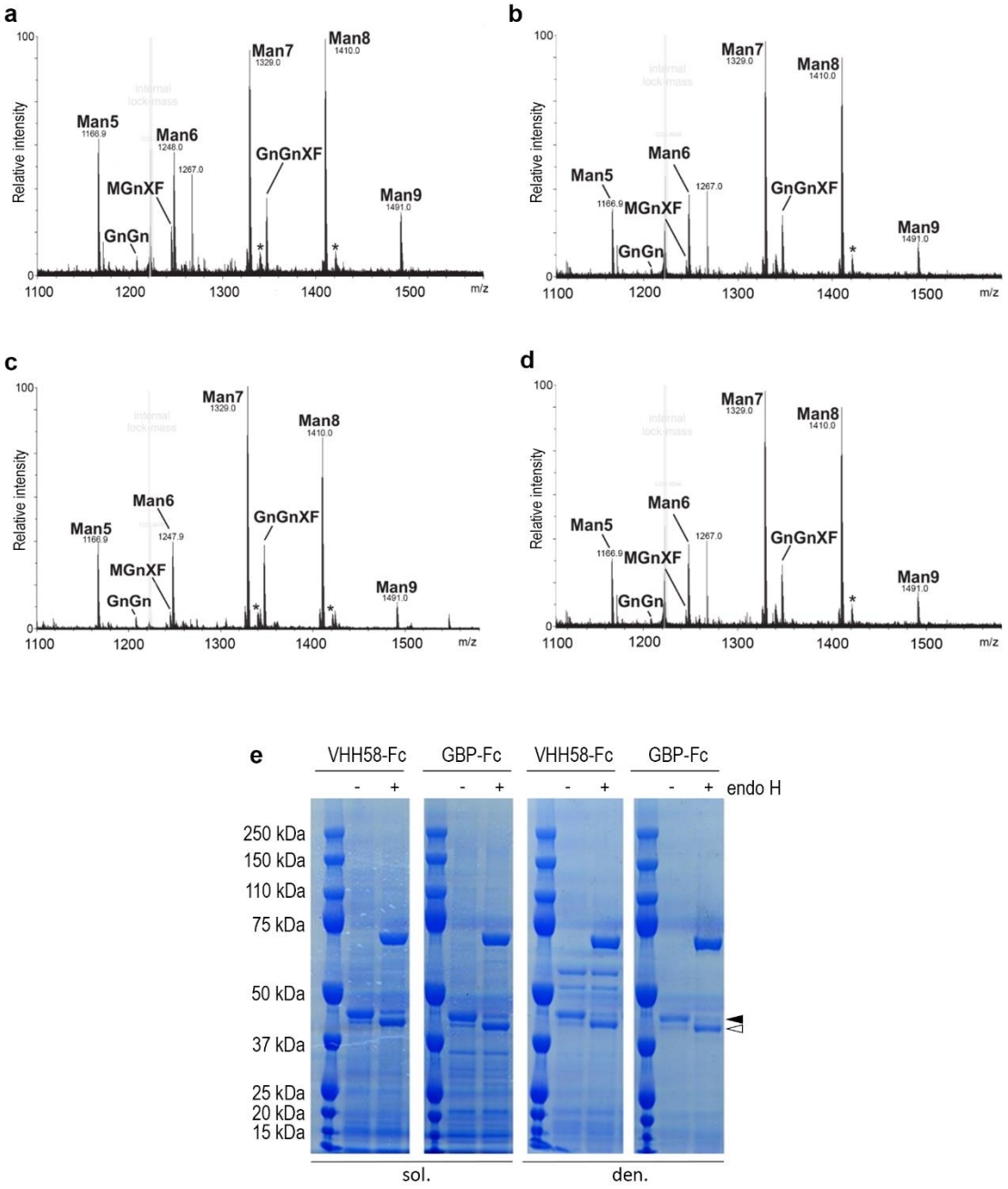

Fig. 2. N-glycan profile and Endo H treatment of soluble and insoluble fractions of seed extracts containing VHH58-Fc or GBP-Fc. **a-d** N-glycan profile of GBP-Fc (**a, b**) and VHH58-Fc (**c, d**) in soluble (**a, c**) and pellet fractions (**b, d**) of seed extracts. Deconvoluted liquid chromatography-mass spectra of the tryptic glycopeptide EAQYNSTFR. G - glucose; A - galactose; M - mannose; F - fucose; X - xylose; Gn - N-acetylglucosamine; See http://www.proglycan.com for an explanation of N-glycan structure abbreviations. **e** Endo H treatment of soluble and pellet fractions of seed extracts containing VHH58-Fc or GBP-Fc. Samples were analyzed on SDS-PAGE under reducing conditions, with (+) and without (-) prior digestion with Endo H. *sol.* soluble seed extract, *den.* pellet re-extracted under denaturing conditions.

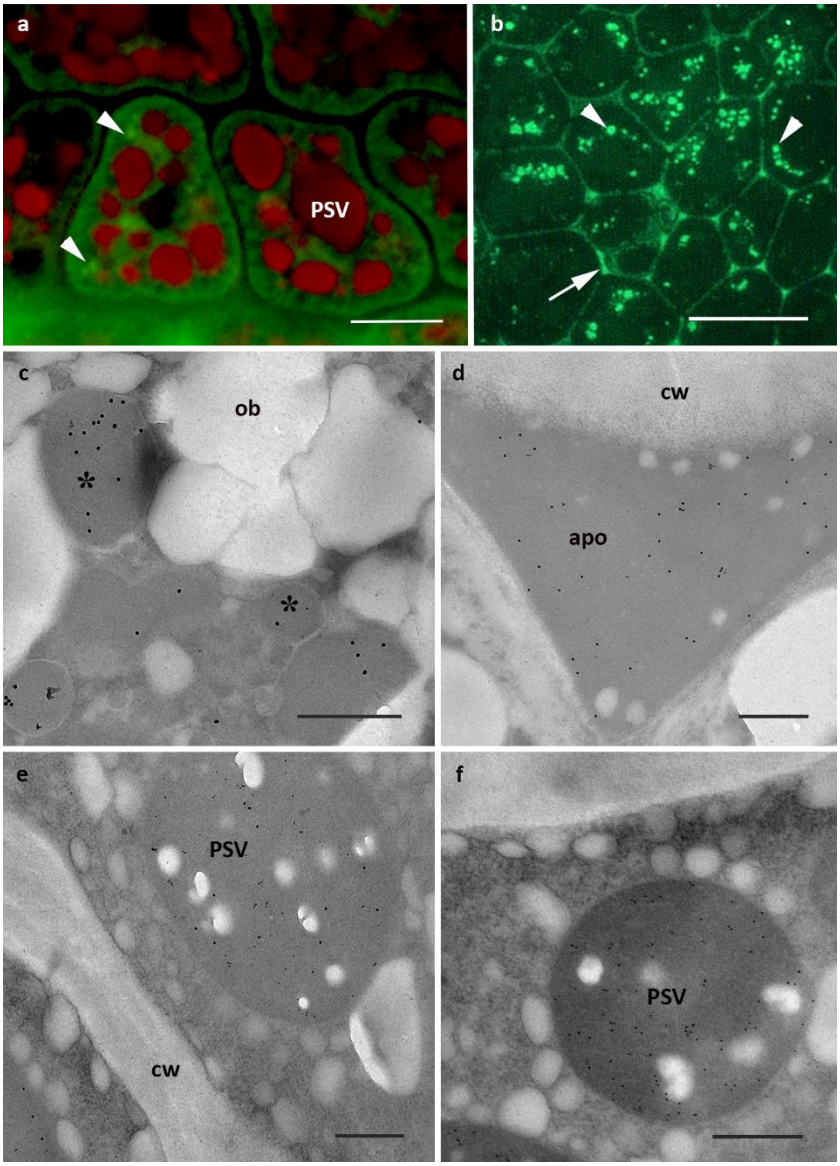

Fig. 3. Localization of GBP-Fc in cotyledon cells of *Arabidopsis* seeds. **a** CLSM with neutral red and ER-Tracker Green™. PSVs appear unaltered. The ER has partially lost the fine network structure, and some aggregates are observed (arrowheads). **b** Localization of GBP-Fc by immunofluorescence microscopy. Strong signals are observed in protein body-like structures within the cytoplasm (arrowheads), and within the apoplast (arrow). **c-f** Co-localization of globulins (10 nm gold) and GBP-Fc (18 nm gold) by TEM. GBP-Fc can be found within ER-derived structures (*, **c**), within the apoplast (apo, **d**) and also within the PSVs (**e**). No significant labeling is detected in any other cell compartment. Globulins (**e**) and albumins (**f**) are found exclusively within the PSVs. Bars 5 µm (**a, b**), 0.5 µm (**c-f**). Apo (apo), cell wall (cw), oil bodies (ob). Representative pictures of the best expressing *Arabidopsis* line are presented in this figure. Pictures of a second line are shown in Supplementary Fig. 4.

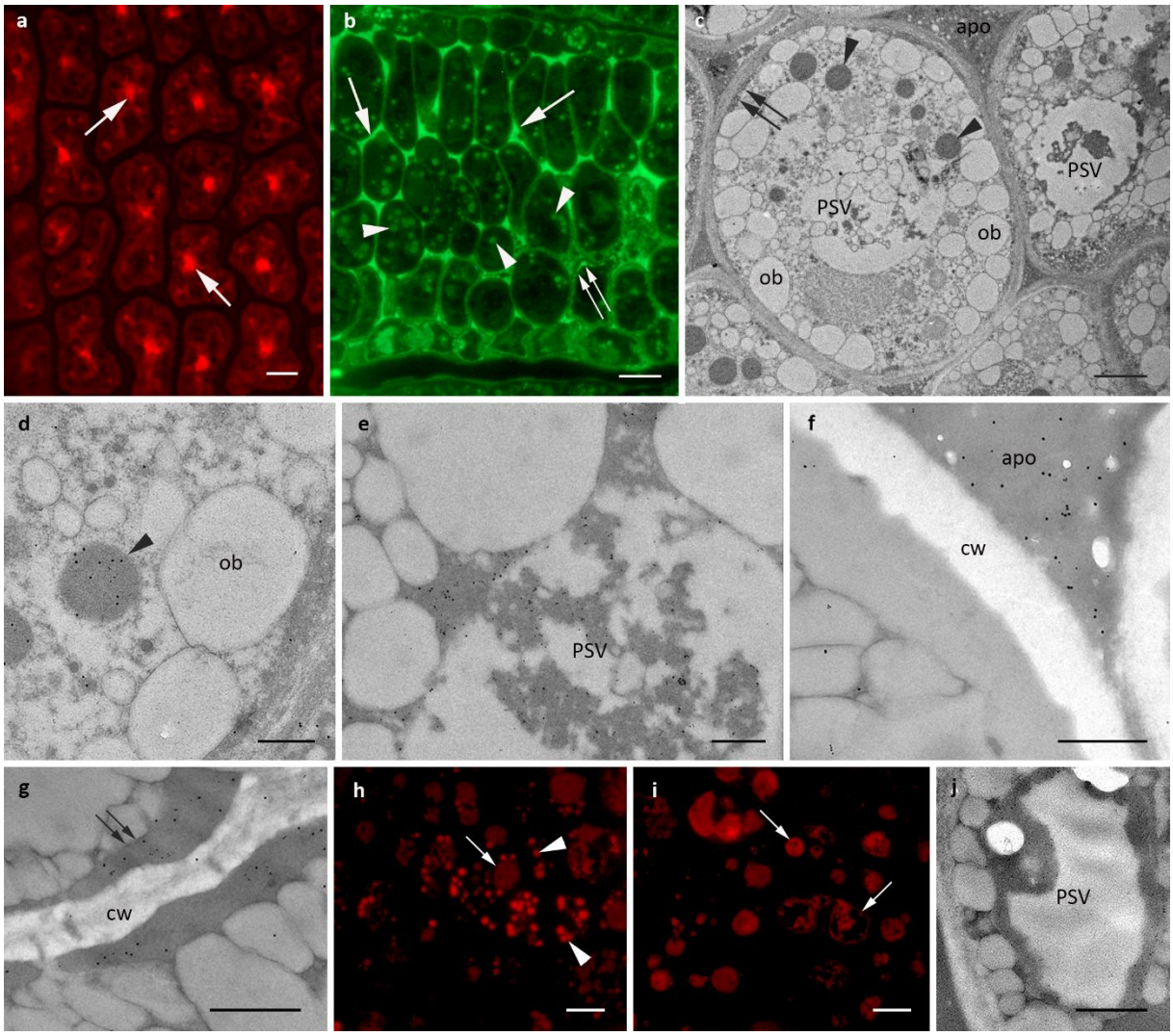

Fig. 4. Localization of VHH-58-Fc in cotyledon cells of *Arabidopsis* seeds. **a** CLSM with neutral red. Positive vacuolar structures are irregular in shape and size (arrows). **b** Localization of VHH58-Fc by immunofluorescence microscopy. A strong signal is present in protein body-like structures within the cytoplasm (arrowheads), within the apoplast (arrows) and also in the periplasmic space (double arrow). **c-g** Co-localization of globulins (10 nm gold) and VHH58-Fc (18 nm gold) by TEM. Membrane-bound structures are very prominent (**c**, arrowheads) and contain abundant gold probes for globulins and VHH58-Fc (**d**, arrowheads). PSVs are almost empty (**c**), but also contain some electron-dense material that is double labeled (**e**). The apoplast appears also clearly double labeled (**f**, apo). Electron-dense material accumulates in the periplasmic space (**c, g**, double arrow) and is decorated with abundant gold probes of both sizes (**g**, double arrow). Apo (apo), cell wall (cw), oil bodies (ob). **h-j** Localization of SSPs by immunofluorescence (**h-i**) and TEM (**j**). Globulins are relocated and found extensively in protein body-like structures (**h**, arrowheads), a minor fraction appears in the PSVs (**h**, arrows). Albumins localize exclusively within the PSV (**i**, arrows; **j**, PSV). Bars 5 µm (**a, b**), 1 µm (**c**), 0.5 µm (**d-g, j**), 10 µm (**h, i**). Representative pictures of the best expressing *Arabidopsis* line are presented in this figure. Pictures of a second line are shown in Supplementary Fig. 5.

SUPPLEMENTARY FIGURES

```
                  *         20          *         40          *         60
VHH28: QVQLQESGGGSVQAGGSLRLSCAFSGDTDSVNVVAWFRQAPGKEREAVAAMNRYGTVKYCADAVKG : 66
VHH58: QVQLQESGGGSVQAGGSLRLSCAASEFALSSVVMAWFRQAPGKECERVASIVGNGRTTY-ADSVKG : 65

            *         80          *        100          *        120          *
VHH28: RFTISQNNAKNTVYLQMNSLKPEDVAIYYCAAARLPD-------SWCSRSDFP-YWGQGTQVTVSS
VHH58: RFIISRDDAKNTVNLQMNSLKVEDTAVYYCAAPRE-----------VVTGVM-CRGRGTQVTVSS
```

Supplementary Fig. 1. VHH28 and VHH58 protein sequences. The CDR 1, 2 and 3 are indicated in bold.

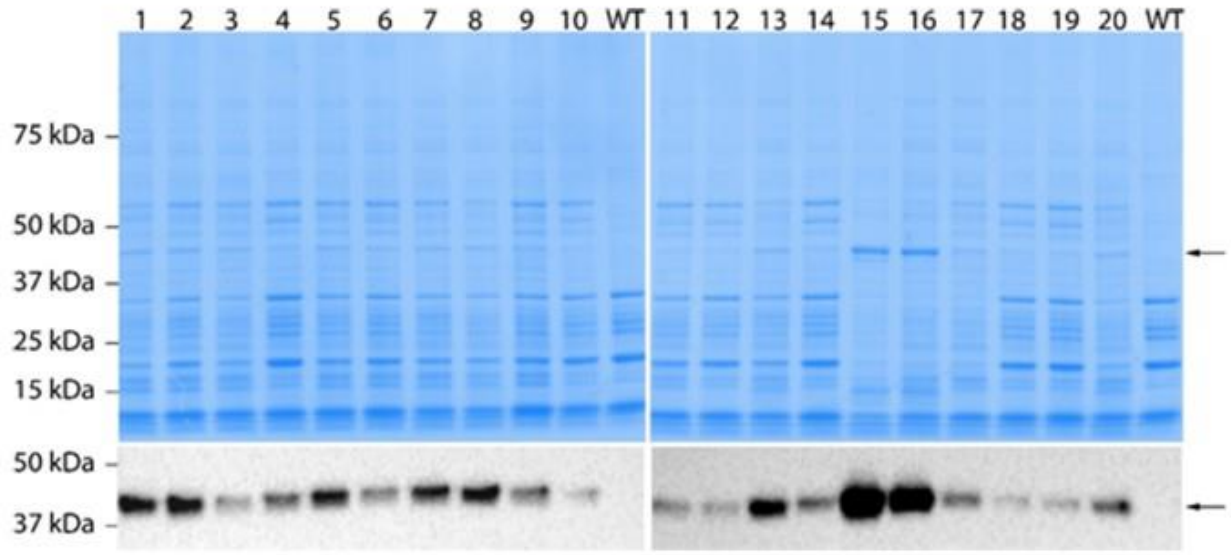

Supplementary Fig. 2. Identification of the highest accumulating VHH58-Fc T2 seed stock among 20 independent transformants. Sixteen µg of protein extract was loaded. VHH58-Fc (arrow) is indicated. Homozygous seeds were generated for line VHH58-Fc_16.

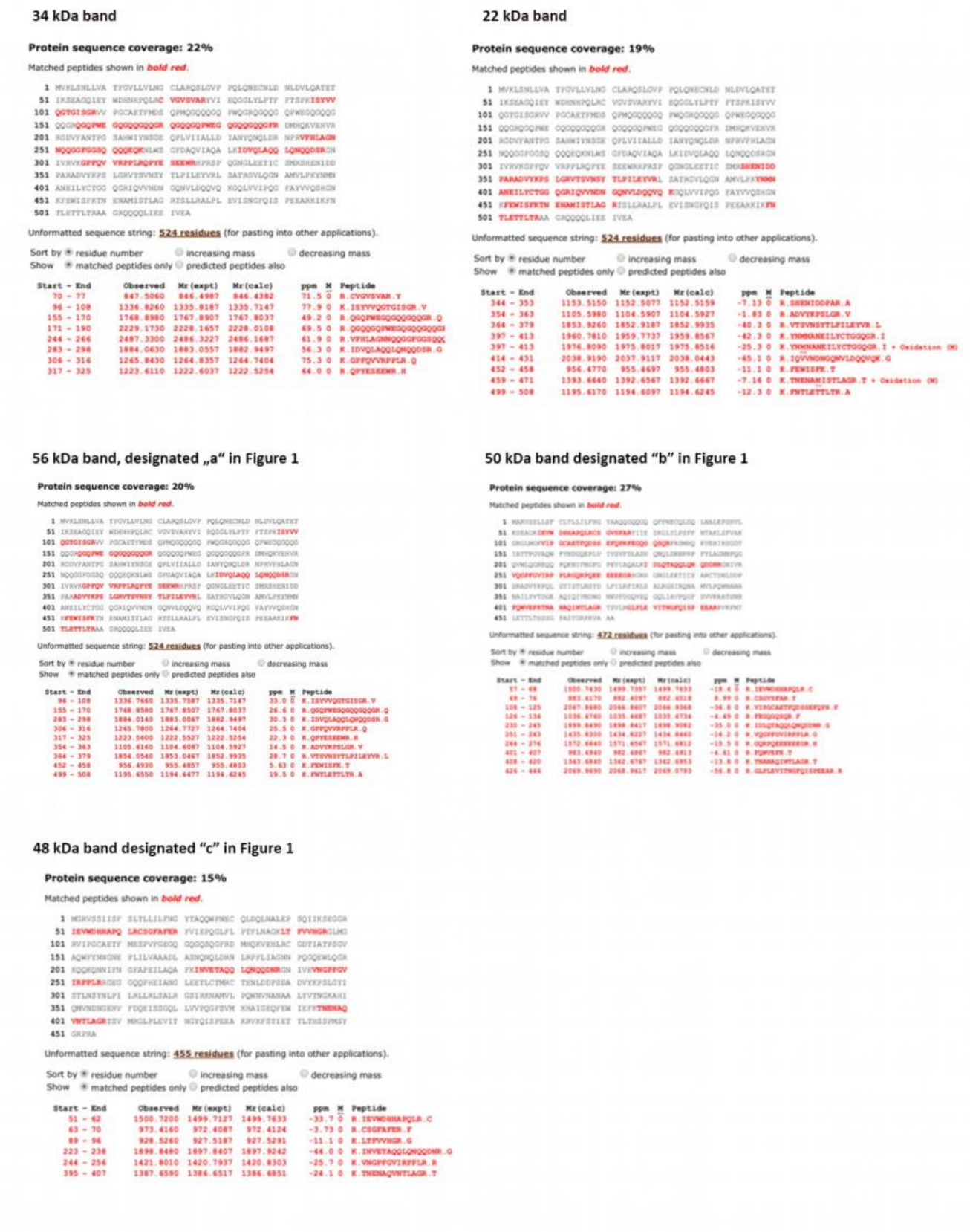

Supplementary Fig. 3. Peptide mass fingerprint of selected bands shown in Fig. 1. The ~34 kDa and the ~22 kDa protein bands in WT extract were identified as alpha and beta chain, respectively, of

Cruciferin C (UniProt ID Q96318). Peptides in the band with the highest molecular mass of ~56kDa (band a) could be assigned to the α and ß subunits of CRU3 (Q96318), identifying the band as CRU3 precursor. Peptides of the ~50kDa band (band b) corresponded to the Cruciferin A1 precursor 12S CRA1 (P15455), and peptides of the ~48kDa band (band c) were assigned to Cruciferin B precursor 12S CRB (P15456).

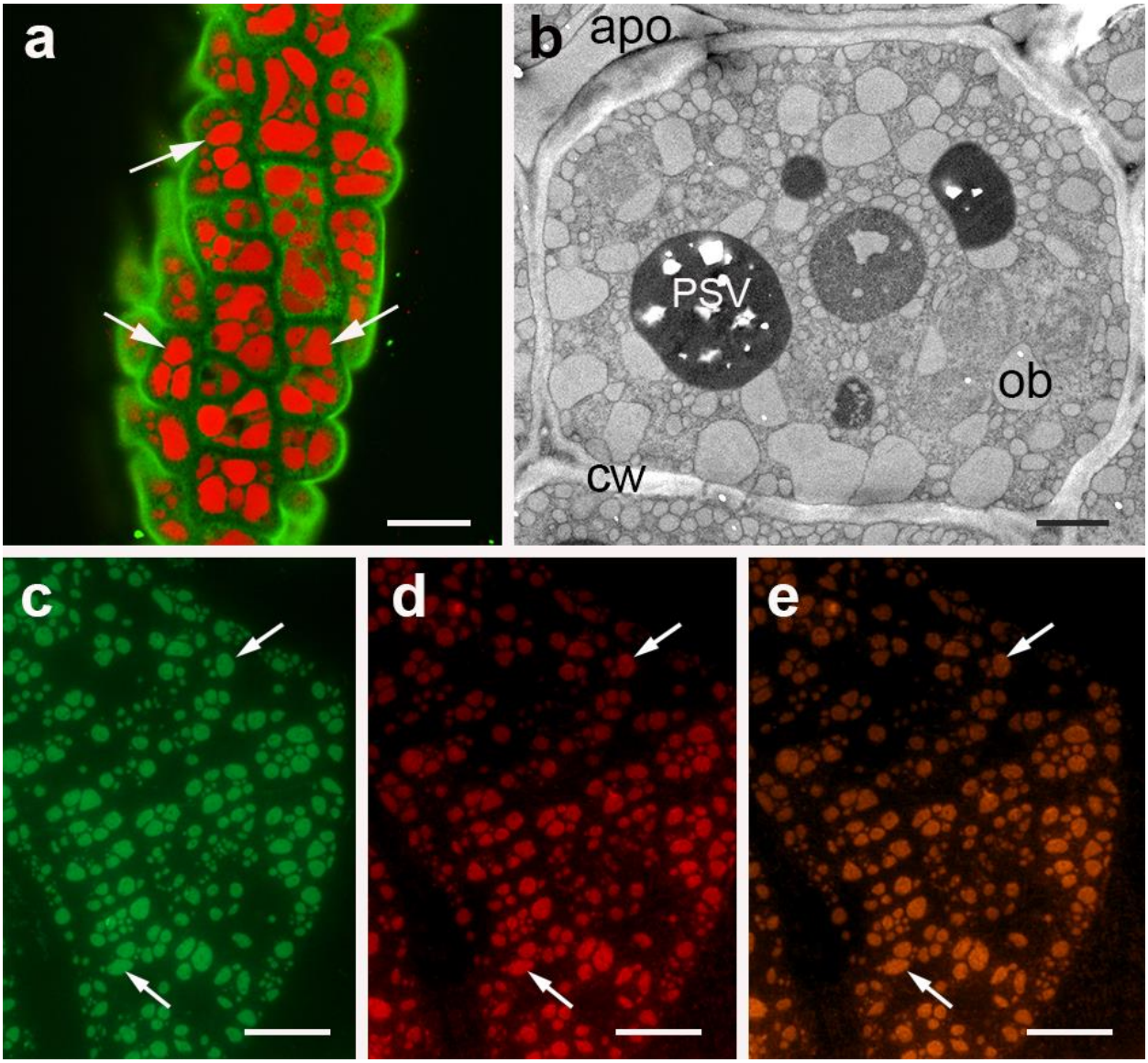

Supplementary Fig. 4. Cotyledon cells of *A. thaliana* WT seeds. **a** Confocal laser scanning microscopy (CLSM) of cotyledon cells containing several protein storage vacuoles (PSVs), clearly highlighted with neutral red (indicated with arrows). Cells were counterstained with ER-Tracker Green™. **b** Transmission electron microscopy (TEM) of the uniformly electron-dense PSV lumen. Apoplast (apo), cell wall (cw) and oil bodies (ob) are indicated. **c-e** Immunofluorescence microscopy showing the localization of globulins (**c**) and albumin (**d**). Both storage proteins co-localize in the PSVs, where they exclusively accumulate (**e**, merged). Bars 5 µm (**a, c-e**), 0.5 µm (**b**).

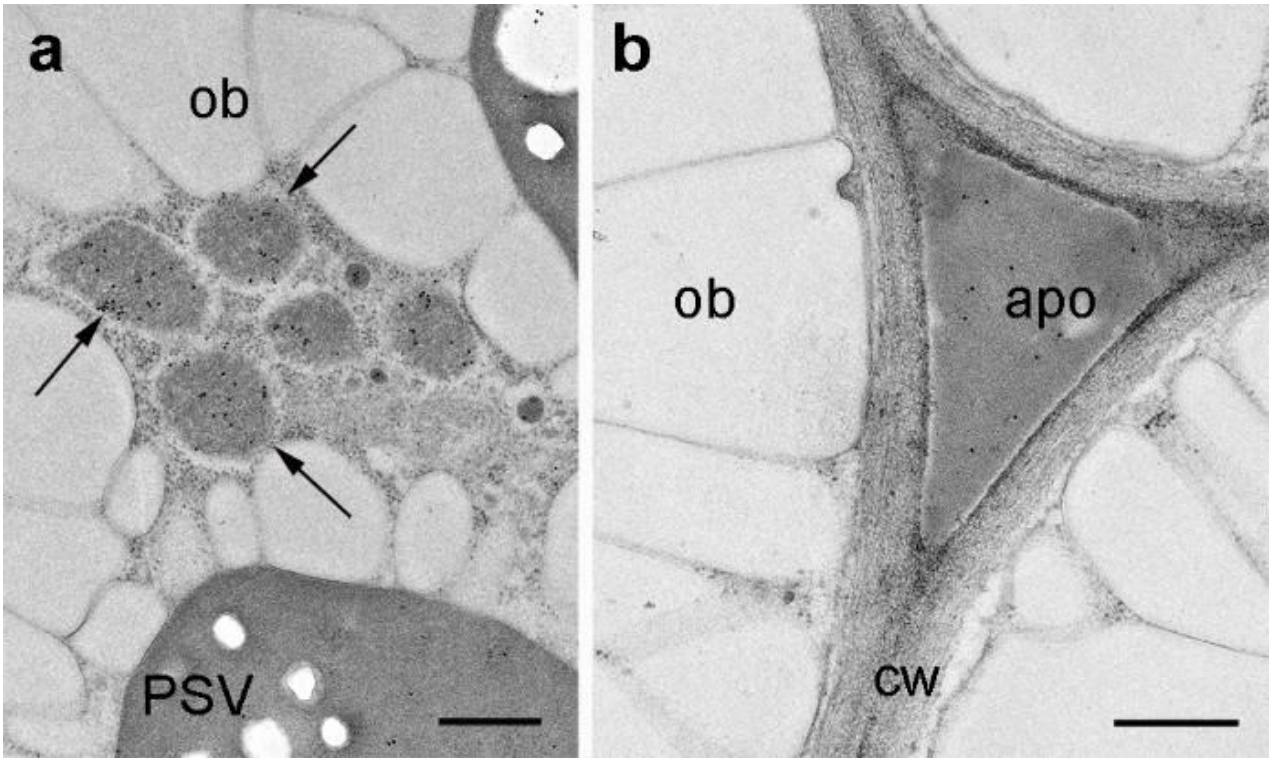

Supplementary Fig. 5. Localization of GBP-Fc in cotyledon cells of Arabidopsis seeds from a second transgenic line. Abundant gold probes within membrane-bound compartments (a, arrows), the PSVs (a) and in the apoplast (b, apo). Cell wall (cw), oil bodies (ob). Bars 0.5 µm.

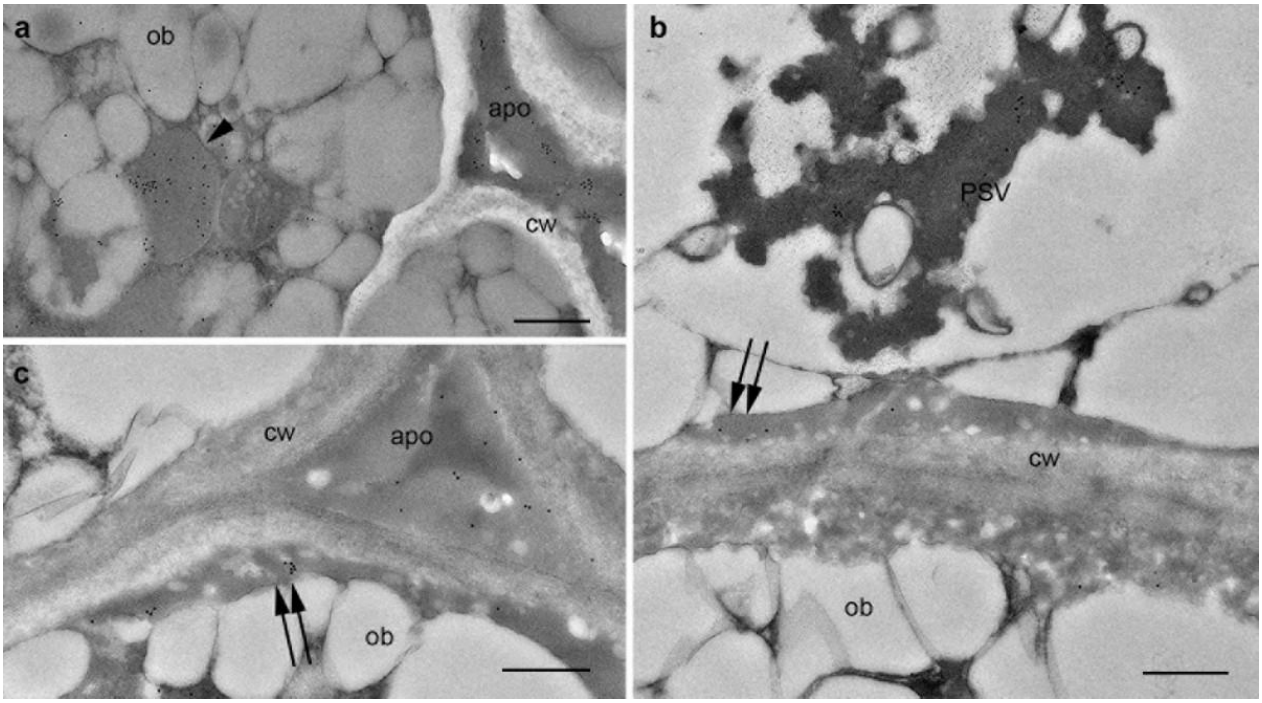

Supplementary Fig. 6. Localization of VHH-58-Fc in cotyledon cells of Arabidopsis seeds of line VHH58-Fc_15. See the abundant labelling in membrane-bound compartments (a, arrowhead) and apoplast (a, c, apo). Gold probes are also found in the PSV remnants (b, PSV). Note also the accumulation of labelled electrondense material between the cell wall and the cell membrane (b, c, double arrow). Cell wall (cw), oil body (ob). Bars 0.5 µm.

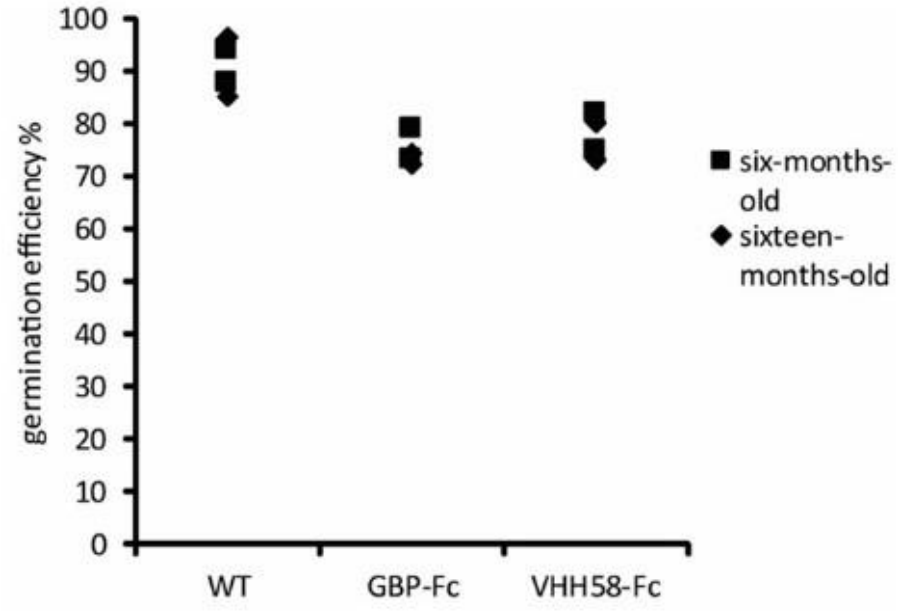

Supplementary Fig. 7. Germination efficiency of GBP-Fc and VHH58-Fc homozygous T4 seed stocks. Germination efficiency was assessed by sowing 100 seeds on non-selective K1 medium.

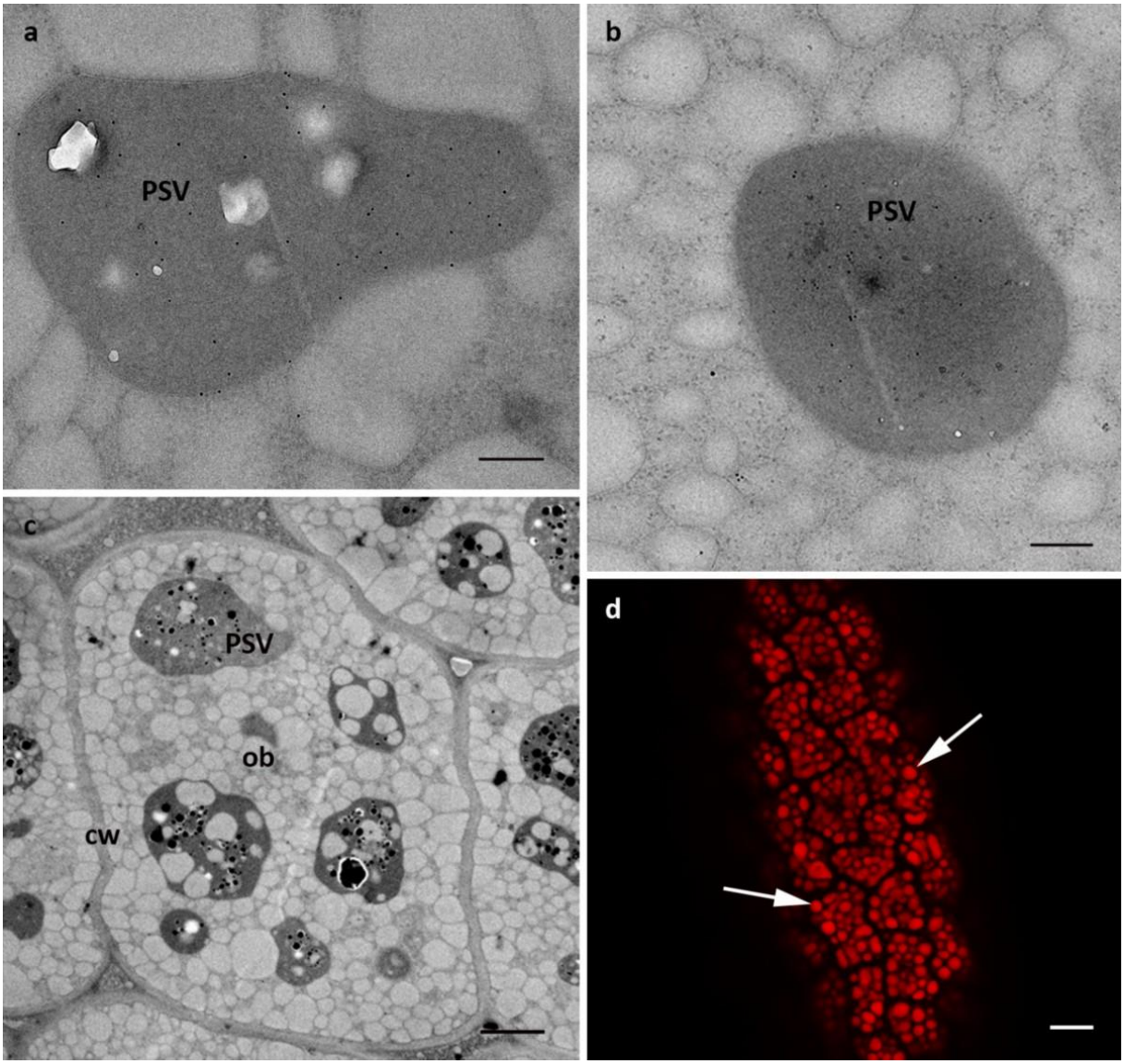

Supplementary Fig. 8. Ultrastructure and immunolocalization of SSP in the *cra1cru2cru3* triple mutant.

(a-c) Transmission electron microscopy (TEM). (d) Confocal laser scanning microscopy (CLSM) Neutral red. Double (a) and triple mutants (b-d).. Albumin is localised within the PSVs, but no gold particles for globulins were observed in both mutants (a, b). PSVs are slightly smaller (for comparison see Figure 3a) but no significant vacuolar phenotype is observed (c, d). Cell wall (cw), oil bodies (ob). Bars 0.25 µm (a, b), 2 µm (c); 10 µm (d).